

## IV.A.9 Novel Sulfur-Tolerant Anodes for Solid Oxide Fuel Cells

Meilin Liu (Primary Contact), Jeng-Han Wang,  
Songho Choi, Zhe Cheng

Georgia Institute of Technology  
School of Materials Science and Engineering  
771 Ferst Drive NW  
Atlanta, GA 30332-0245  
Phone: (404) 894-6114; Fax: (404) 894-9140  
E-mail: meilin.liu@mse.gatech.edu

DOE Project Manager: Briggs White

Phone: (304) 285-5437  
E-mail: Briggs.White@netl.doe.gov

### Objectives

- Characterize the sulfur-poisoning effect on anode-supported solid oxide fuel cells (SOFCs) under practical operation conditions
- Investigate the sulfur-anode interaction mechanism in H<sub>2</sub>S contaminated fuels at elevated temperatures
- Establish an effective operational window that allows SOFCs to reach lifetime targets in commercially viable power generation environments
- Modify Ni-YSZ (yttria-stabilized zirconia) anode surface to achieve enhanced sulfur tolerance

### Accomplishments

- Revealed sulfur poisoning mechanism and the effects of cell operating conditions (including temperature and H<sub>2</sub>S concentration) on sulfur poisoning and recovery of nickel-based anodes in SOFCs.
- Predicted a new S-Ni phase diagram with a region of sulfur adsorption on Ni surfaces, corresponding to sulfur poisoning of Ni-YSZ anodes under typical SOFC operating conditions.
- Established the “standard” Raman spectra for several nickel sulfides commonly observed in sulfur poisoning of Ni-based anodes and verified the characteristic Raman shifts using density functional theory (DFT) calculations.
- Designed and constructed a multi-cell testing system capable of simultaneously performing electrochemical tests of 12 button cells in fuels with four different concentrations of H<sub>2</sub>S.
- Achieved modification of the Ni-YSZ anode surface using a thin coating of Nb<sub>2</sub>O<sub>5</sub> to enhance sulfur tolerance.

### Introduction

SOFCs have a great potential to be one of the cleanest, most efficient and versatile systems that convert chemical energy to electrical energy. One of the unique advantages of SOFCs over other types of fuel cells is the capability of direct utilization (sometimes through internal reforming) of hydrocarbon fuels. Unfortunately, many hydrocarbon fuels contain sulfur, which may dramatically degrade SOFC performance even at very low levels. Low concentrations of sulfur are difficult to remove efficiently and cost-effectively. Therefore, knowing the exact poisoning process for state-of-the-art cells with Ni-YSZ supporting anodes, understanding the detailed anode poisoning mechanism, and developing new sulfur-tolerant anodes are essential for the promotion of SOFCs that run on hydrocarbon fuels.

The current project focuses on (i) characterizing both the short-term and long-term sulfur poisoning process for state-of-the-art SOFC button cells with a anode-supported structure, (ii) investigating the sulfur poisoning mechanism for the Ni-based anode via experiments and theoretical calculations, and (iii) developing new anode materials and/or architectures that provide enhanced sulfur tolerance.

### Approach

In theoretical analysis, quantum chemical calculations with thermodynamic correction were used to predict the interactions between H<sub>2</sub>S-contaminated hydrogen fuel and Ni surfaces under SOFC operation conditions. The vibrational frequencies and modes of several nickel sulfides were computed using finite displacement approach to assist the interpretation of Raman spectra obtained from experiments. The electronic structures of these sulfides were also calculated and correlated with the poisoning behavior.

On the experiment side, a multi-cell testing system was designed and constructed in our lab, consisting of a high temperature furnace, a gas distribution system, and a 12-channel electrochemical testing station. Meanwhile, the surfaces of Ni-YSZ anodes were modified with a thin film of other materials to improve the sulfur tolerance. Fuel cells with dense Ni-YSZ anodes were fabricated using a co-sintering method in a reducing atmosphere. A thin film of Nb<sub>2</sub>O<sub>5</sub> was then deposited on the anode surface by sputtering. The power output and the interfacial impedance response were recorded as a function of time upon exposure to hydrogen with or without 50 ppm H<sub>2</sub>S.

## Results

Shown in Figure 1 is a new S-Ni phase diagram constructed from quantum chemical calculations with thermodynamic corrections. This phase diagram suggests that a clean Ni surface (in the white region) will first adsorb sulfur atoms when exposed to a small amount of  $H_2S$ , crossing the blue line and entering the blue (middle) region. The surface coverage of nickel by sulfur increases as the temperature is reduced until the surface is completely covered by sulfur (approaching the red line between the blue and the yellow region) before the formation of  $Ni_3S_2$  (in the yellow region). The blue region can not be predicted directly from the classical thermodynamic database and, thus, is missing from the existing S-Ni phase diagram [1]. The important implication of the calculated phase diagram is that it can be used to accurately predict the conditions to avoid sulfur poisoning (in the white region) and to explain existing measurements [2]. These results also suggest that sulfur poisoning is due to the adsorption of sulfur atoms on the nickel surface, which blocks active sites for fuel oxidation.

Listed in Table 1 are the Raman frequencies of four nickel sulfide species (i.e.,  $Ni_3S_2$ , NiS,  $Ni_3S_4$ , and  $NiS_2$ ) determined from DFT calculations as well as

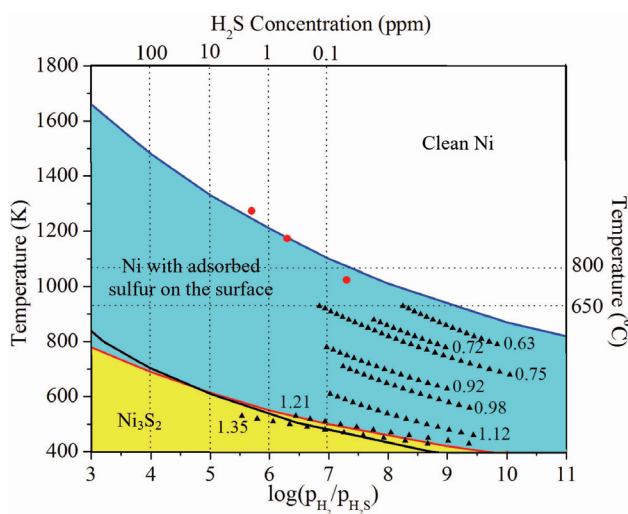


**FIGURE 1.** Calculated phase diagram for the S-Ni system in  $H_2S/H_2$  fuel mixtures. The white, blue, and yellow regions represent clean Ni phase without adsorbed sulfur on the surface, Ni phase with adsorbed sulfur on the surface, and  $Ni_3S_2$  bulk phase, respectively. The blue line is the calculated phase boundary between clean Ni surface and Ni surface with adsorbed sulfur; the red line is the calculated phase boundary between Ni surface with adsorbed sulfur and  $Ni_3S_2$  bulk phase; the black line is phase boundary between bulk nickel and  $Ni_3S_2$  determined by experiments [1]. The black triangles are data points for the sulfur chemisorption isosteres on Ni surface with different surface coverage [3]. The red circles represent the experimentally determined critical  $H_2S$  concentration values above which the sulfur poisoning of fuel cell anode became significant [2].

**TABLE 1.** The Raman Vibrational Frequencies ( $cm^{-1}$ ) Determined by Theoretical Calculations and Experiments for  $Ni_3S_2$ , NiS,  $Ni_3S_4$  and  $NiS_2$

Material	Modes	Calculated	Experiment
$Ni_3S_2$	E(1)	367, 367	351
	$A_1(1)$	320	325
	E(2)	317, 316	303
	E(3)	241, 241	223
	E(4)	204, 203	201
	$A_1(2)$	201	189
NiS	$A_1(1)$	356	370
	E(1)	341, 341	349
	$A_1(2)$	290	300
	$A_1(3)$	254	
	E(2)	252, 251	246
	E(3)	231, 230	
	E(4)	201, 201	
	E(5)	148, 148	
$Ni_3S_4$	$A_{1g}(1)$	388	375
	$T_{2g}(1)$	339, 338, 338	335
	$T_{2g}(2)$	284, 284, 283	285
	$E_g(1)$	208, 207	222
	$T_{2g}(3)$	206, 206, 205	
$NiS_2$	$T_g(1)$	462, 462, 461	489
	$A_g(1)$	446	479
	$T_g(2)$	342, 341, 341	
	$E_g(1)$	285, 285	285
	$T_g(3)$	278, 278, 277	273

from Raman measurements. The computed vibrational frequencies are generally in good agreement with Raman spectra obtained by experiments (with deviation of less than <10%) and can be used to identify nickel sulfides in our sulfur poisoning studies. The significance of the theoretical calculations is that previous studies on the nickel sulfide Raman spectra often contradicts one another, which makes it impossible to use any of them as a reliable reference.

Shown in Figure 2 is a picture of the multi-cell testing system built in our lab. The multi-cell system is capable of simultaneously testing 12 button cells under various electrochemical conditions (e.g., potentiostatic, galvanostatic, or potentiodynamic conditions) at a temperature up to 1,050°C. The gas distribution system can delivery gas mixtures from humidified inert gas (e.g.,  $N_2$ ), fuel (e.g.,  $H_2$ ), and  $H_2S$  containing fuels. It can supply up to four different fuel mixtures with  $H_2S$  concentration varying from 0.05 to 100 ppm.



**FIGURE 2.** The Multi-Cell Testing System Consisting of a High Temperature Furnace, a Gas Distribution System, and a 12-Channel Electrochemical Testing System

Shown in Figure 3 are the electrochemical measurements on cells having a structure of Pt/YSZ/dense Ni-YSZ with or without  $\text{Nb}_2\text{O}_5$  coating in dry  $\text{H}_2$  at  $700^\circ\text{C}$ . In Figure 3(a), the increased power density (from 23 to  $49 \text{ mW/cm}^2$  for the cell with a  $\text{Nb}_2\text{O}_5$  coating) indicates that  $\text{Nb}_2\text{O}_5$  enhanced cell performance after (partially) reduced in  $\text{H}_2$ . This is also supported by the impedance data shown in Figure 3(b); the interfacial resistance decreased from  $15 \Omega\text{-cm}^2$  for the cell without  $\text{Nb}_2\text{O}_5$  coating to  $7 \Omega\text{-cm}^2$  for the cell with a  $\text{Nb}_2\text{O}_5$  coating. Shown in Figure 3(c) is the stability of the cell with a  $\text{Nb}_2\text{O}_5$  coated anode exposed to 50 ppm  $\text{H}_2\text{S}$  at  $700^\circ\text{C}$ . The current density dropped slightly as  $\text{H}_2\text{S}$  was first introduced, but quickly recovered to the same value as in  $\text{H}_2$  fuel. The cell with  $\text{Nb}_2\text{O}_5$  coating showed stable performance in fuel with 50 ppm  $\text{H}_2\text{S}$  for 12 h.

### Conclusions and Future Directions

The effective operational windows have been identified from the computed Ni-S phase diagram, which can distinguish the clean Ni surface, the Ni surfaces

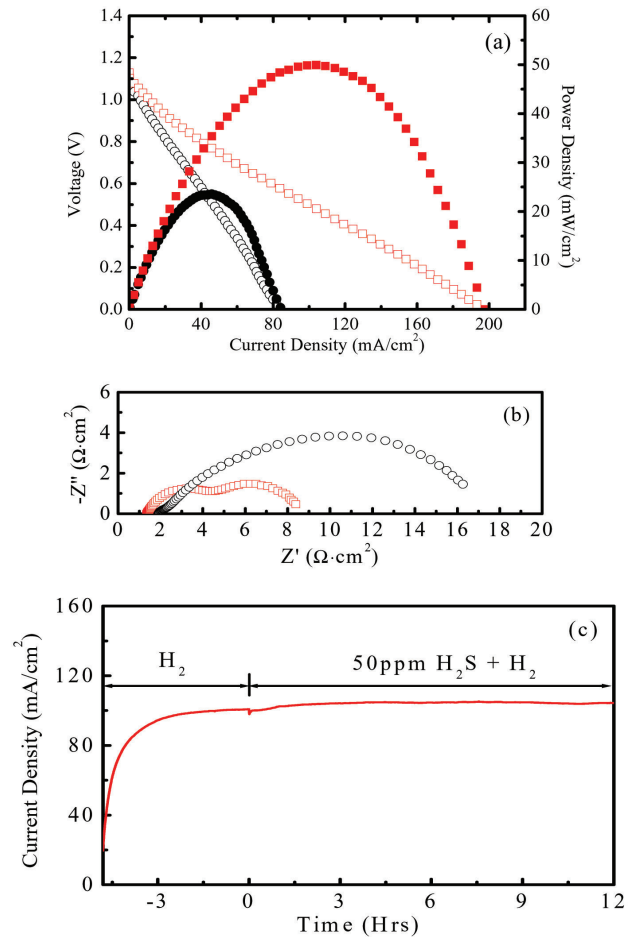


**FIGURE 3.** (a) Current-voltage relationship and power output and (b) impedance spectra for cells (Pt/YSZ/dense Ni-YSZ tri-layer structure) with (squares in red) and without (circles in black)  $\text{Nb}_2\text{O}_5$  coating in dry  $\text{H}_2$  at  $700^\circ\text{C}$ , and (c) the change in current density for the cell with a  $\text{Nb}_2\text{O}_5$  coating over the dense Ni-YSZ anode in dry 50 ppm  $\text{H}_2\text{S}$  balanced with  $\text{H}_2$  at  $700^\circ\text{C}$ .

partially covered with adsorbed sulfur atoms, and bulk nickel sulfide  $\text{Ni}_3\text{S}_2$ . A multi-cell testing system has been built: it enables simultaneous testing of up to 12 cells and can greatly increase the experiment output. The vibrations at the  $\Gamma$ -point of the sulfides are computed and confirmed with Raman measurements. Finally, the  $\text{Nb}_2\text{O}_5$  coated Ni-YSZ anode showed promising sulfur tolerance in 50 ppm  $\text{H}_2\text{S}$  contaminated fuels.

Future work is briefly outlined as follows:

- Characterize both the short-term and long-term sulfur-poisoning effect for anode-supported SOFC button cells under various current density and  $\text{H}_2\text{S}$  concentrations.
- Optimize the surface modification process to achieve enhanced sulfur tolerance while maintaining reasonable cell performance and stability.

## FY 2007 Publications/Presentations

1. Z. Cheng, S. Zha, and M. Liu, "Stability of Materials as Candidates for Sulfur-Resistant Anodes of Solid Oxide Fuel Cells," *Journal of The Electrochemical Society*, **153**, A1302-A1309 (2006).
2. Y. M. Choi, C. Compson, Charles, M. C. Lin, M. Liu, "A mechanistic study of H<sub>2</sub>S decomposition on Ni- and Cu-based anode surfaces in a solid oxide fuel cell," *Chemical Physics Letters*, **421**, 179-183 (2006).
3. J. Dong, Z. Cheng, S. Zha, and M. Liu, "Identification of Nickel Sulfides on Ni-YSZ Cermet Exposed to H<sub>2</sub> Fuel Containing H<sub>2</sub>S Using Raman Spectroscopy," *Journal of Power Sources*, **156**, 461-465 (2006).
4. Y. M. Choi, C. Compson, M.C. Lin, and M. Liu, "Ab initio analysis of sulfur tolerance of Ni, Cu, and Ni-Cu alloys for solid oxide fuel cells," *Journal of Alloys and Compounds*, **427**, 25 (2007).
5. S. Zha, Z. Cheng, and M. Liu, "Sulfur Poisoning and Regeneration of Ni-based Anodes in Solid Oxide Fuel Cells," *Journal of The Electrochemical Society*, **154**, B201 (2007).
6. Z. Cheng, M. Liu, "Characterization of Sulfur Poisoning of Ni-YSZ Anodes for Solid Oxide Fuel Cells Using *in situ* Raman Microspectroscopy," *Solid State Ionics*, **178**, 925, 2007.
7. J. H. Wang, M. Liu, "Prediction of Ni-S Phase Diagram using DFT Calculations and Thermodynamic Corrections," *Electrochemistry Communications*, in press.
8. J. H. Wang, Z. Cheng, J.-L. Bredas, M. Liu, " Electronic and Vibrational Properties of Nickel Sulfides: A Density Functional Theory Study," *Journal of Physical Chemistry C*, submitted.
9. J. H. Wang, M. Liu, "Computational Study of Surface Regeneration of Sulfur-Poisoned Ni surface under SOFC Operation Conditions by First-Principles and Thermodynamic Calculations," *Journal of Physical Chemistry C*, submitted.

## References

1. T Rosenqvist: J. Iron Steel Inst. 176 (1954) 37.
2. Y Matsuzaki, I Yasuda: The poisoning effect of sulfur-containing impurity gas on a SOFC anode: Part I. Dependence on temperature, time and impurity concentration. Solid State Ionics 132 (2000) 261.
3. JG McCarty, H Wise: Thermodynamics of sulfur chemisorption on metals. I. Alumina-supported nickel. J. Chem. Phys. 72 (1980) 6332.